DSC North America 2003 Proceedings, Dearborn, Michigan, October 8-10, 2003 (ISSN 1546-5071).

MOTION DRIVE ALGORITHMS AND SIMULATOR DESIGN TO STUDY MOTION EFFECTS ON INFANTRY SOLDIERS

Harry J. Zywiol, Jr., U.S. Army Tank-Automotive Research Development and Engineering Center (TARDEC), Warren, MI, 48397. Tel - 586-574-5032. zywiolh@tacom.army.mil

Dr. Richard Romano, Realtime Technologies Incorporated, Clawson, MI. Tel – 248-705-0705. romano@simcreator.com

ABSTRACT

Army vehicle and system developers need to mitigate potential problems of motion sickness described by Cowings, Toscano, DeRoshia, & Tauson, [1] and ensure that crewstation designs are optimized in their adaptation to the soldier. Using a motion base simulator, Engineers and Scientists at the U.S. Army Tank-Automotive Research, Development, and Engineering Center, TARDEC, have begun a program to study motion effects on soldiers who are transported in infantry carriers in extended road marches.

Several experiments are being designed and configured on the TARDEC National Automotive Center (NAC) Ride Motion Simulator (RMS) that recreate the proving ground environment in the laboratory to permit further study of motion sickness symptoms, their affects on soldier performance, and eventually mitigation techniques. The RMS is capable of high-transient motion dynamics to give the occupant very realistic mobility cues. This paper describes the motion drive algorithm and simulator configuration for the first of these soldier studies. Motion data was recorded on a combat vehicle at a US Army proving ground. These data were transformed and preprocessed using a motion drive algorithm into motion drive data for the 6 DOF simulator. By preprocessing the motion data with a non stationary linear quadratic optimal motion drive algorithm it was found that substantial specific forces cues could be recovered using tilt coordination and linear motion of the base.

INTRODUCTION

The U.S. Army's Future Combat System (FCS) program [2] will develop network centric concepts for a multi-mission combat system that will be overwhelmingly lethal, strategically deployable, self-sustaining and highly survivable in combat through the use of an ensemble of manned and unmanned ground and air platforms. Of particular interest to the driving simulator community is that the FCS Operational Requirements Document states two requirements must be met. The first requirement states that Army operations are performed "on-the-move." The second states that these "on-the-move" operations be performed "without adverse effects." In the past, command and control operations were usually performed in a stationary vehicle. Typical operations could include surveillance, gathering intelligence information, or route planning. However, in the near future, these operations will have to be performed in a moving vehicle environment in order to maintain a swift operational tempo. The concern among human factors specialists is that adverse effects on soldiers will increase unless new vehicle crewstation designs address these command and control issues with a proven soldier/machine interface.

TARDEC Ride Motion Simulator

The Ride Motion Simulator described by Nunez, Paul, and Brudnak [3], is being configured to study motion effects on infantry soldiers. A photograph of the simulator is shown in Figure 1.

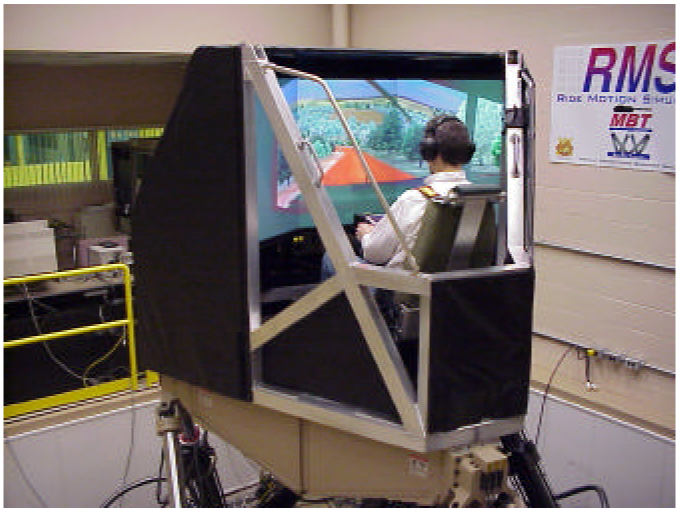

FIGURE 1 Ride Motion Simulator

The simulator features an electro-hydraulic 6 degree of freedom table on which a vehicle cab structure can be mounted. A re-configurable cab supports one occupant. The simulator can be outfit with displays driven by a real-time image generator, driving controls, and an audio generation system. Simulations can be built using paved road or cross country visual and terrain databases, coupled with multi-body vehicle dynamics models traversing these databases.

Simulator experiment designs

Currently, there are three experiment designs being set up using the Ride Motion Simulator that begin to address the FCS on the move and adverse effects requirements. These are briefly described here:

Indirect driving versus Head Mounted Display (HMD) driving. *Indirect* driving is a design where the vehicle driver views are portrayed on display screens rather than *directly* looking through windshields or vision blocks. Vehicle cameras, appropriately placed, produce an image of the outside environment that is displayed on a screen for the vehicle driver. Indirect vision systems can result in a vehicle designs that are safer for the crew since a direct line of sight for the driver is not required. Head mounted displays, for driving purposes, carry the indirect display one step further in that the driver is more immersed in the scene. Data can be displayed within the scene as well as providing the driver with additional navigation or other information. A head or eye tracker can render the scene per the direction of this head or eyes.

Indirect driving in a tele-operations mode. Army researchers are exploring the ground vehicle simulation design for use in robotic applications and other tasks. Tele-operating an unmanned ground vehicle (UGV) when both control and robotic vehicle are in motion presents a number of challenges for the control operator. This is because the operator is continuously experiencing different and therefore conflicting visual and motion cues. The tele-operation task coupled with command and control tasks could present situations too difficult for the soldier to handle.

Effects on infantry soldiers in a road march environment. Typically, a squad of about nine soldiers will be confined in the rear of an infantry carrier during a road march of several hours. The soldiers have no periscopes or view of the outside world. Soldiers have known to become disoriented and ill, especially when they are asked to conduct command and control functions. The RMS is being configured to replicate the motion and vibration road march environment so that it can be accurately presented to soldiers in a laboratory environment. Studies will be performed to measure how well each soldier performs various infantry tasks as they exit (dismount) from the simulator.

SIMULATOR CONFIGURATION AND DATA PROCESSING

Proving ground data collection

TARDEC recently seized an opportunity to obtain some data that was collected at the U.S. Army Proving Ground in Aberdeen Maryland. The goal of the data collection was to validate the RMS as a tool for human performance testing. The data were recorded off a new, eight-wheeled, combat vehicle called the Stryker, shown in Figure 2.

FIGURE 2 Stryker vehicle

The Infantry Fighting Vehicle variant of the Stryker will transport a squad of nine soldiers, with their equipment, to and around the battlefield. In short, they must be ready to perform physical (e.g., lifting, sustained load carriage), psychomotor (e.g., balance, eye-hand coordination), perceptual (e.g., accurately hearing and seeing), and cognitive (time and accuracy of responding to information) tasks. [4]

The Stryker vehicle squad was tested at the proving ground in Maryland for a number of these crew measures while traversing two courses: Perryman A and Perryman 1. These courses are characterized as secondary, gravel roads, with wide and narrow turns. They are both flat with numerous turns, although soil types differ slightly. The surface roughness of Perryman A is 8.9mm (.35 inch) rms and Perryman 1 is 10.4 mm (.41 inch) rms. The Perryman A and Perryman 1 courses are 3840 meters (2.4 miles) and 8320 meters (5.2 miles) in length respectively.

Vehicle speeds on these courses are typically 25 to 57 kph (15 to 35 mph). A number of signals were recorded from sensors mounted to the vehicle. These signals are: vehicle speed, vehicle body rate in pitch, roll, and yaw, vehicle linear acceleration in lateral, longitudinal, and vertical. Channels measuring audio and sound pressure level were also recorded from within the vehicle. The signals were digitally sampled at 500 samples per second at the proving ground and are described in Table 1.

TABLE 1 Proving ground data description

Channel number	Description	Low Pass freq. (hz)	Units
1	(V) Seat bottom accel	100	G's
2	(T) Seat bottom accel	100	G's
3	(L) Seat bottom accel	100	G's
4	Road Speed	100	mph
5	Yaw rate – motion pak	100	Deg/sec
6	Roll rate – motion pak	100	Deg/sec
7	Pitch rate – motion pak	100	Deg/sec
8	(T) motion pak accel	100	G's
9	(L) motion pak accel	100	G's
10	(V) motion pak accel	100	G's

It is desired to determine how well the RMS can replicate the one-hour road march motion environment as experienced at the proving ground. The RMS cab will be configured similarly as the interior of the Stryker carrier. See Figure 3. A bench-type seat with seat back and lap belt will be installed. Because the RMS cab is not large enough to install an entire squad cab, the video screens inside the RMS cab will display still photographs of the interior of the Stryker. A canvas shroud will be placed such that the soldier will not be able to see the outside laboratory environment. The RMS motion controller has been tuned to deliver high bandwidth motion drives in excess of 25 hertz.

FIGURE 3 Interior view of Stryker vehicle compartment

Experiment plan.

An experiment using the Ride Motion Simulator is being considered. It will replicate some of the Proving Ground conditions in an attempt to validate using the simulator for future vehicle on-the-move efforts. Twelve rifle-qualified infantry soldiers will be tested in the simulator. Each soldier will be subjected to the following:

- 1 hour road march in motion simulator
- dismount from simulator
- walk on narrow wooden rails. The soldiers' balance ability will be recorded.
- Rifle shooting using indoor firing simulator. The soldiers' firing performance will be recorded.
- Motion sickness and cognitive questionnaires will be administered

PREPROCESSING THE DATA FOR THE SIMULATOR

Washout algorithms are used in driving simulators to translate the large motions of the actual vehicle into the limited motion envelope of the motion base. Washout algorithms have been developed for flight simulation over the past several decades and several different approaches have been considered; a review of these approaches is given by Reid and Nahon [5]. The first set of motion control logic algorithms to be widely used is now called the classical algorithms. They use high-pass filters to eliminate the low frequency, high-amplitude motions of the vehicle. They also provide tilt coordination in order to recover some of the low-frequency acceleration cues lost due to the high frequency filtering. The selection of the parameters for the digital filters is a trade-off between maximizing cue recovery while eliminating motion commands that are outside the envelope of the motion base. A number of researchers have developed and evaluated the classical algorithm [6-9]. The classical algorithm is shown in Figure 4.

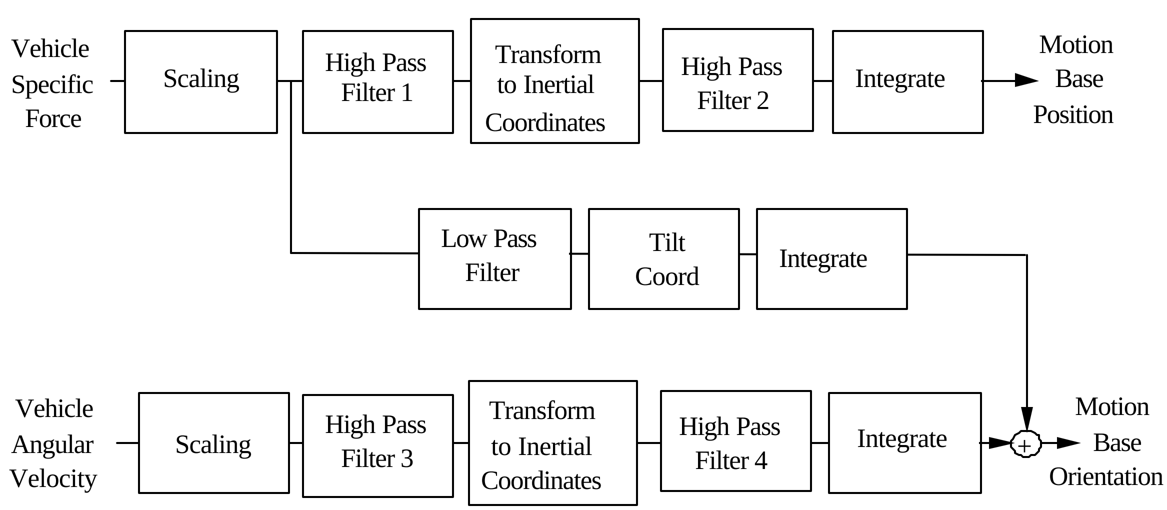

FIGURE 4 Classical Algorithm

Due to the trade-off in tuning the digital filters, another algorithm that is used widely in flight simulation is the coordinated adaptive algorithm. The flow of this algorithm is quite similar to that of the classical algorithm however in this case the scaling factors, and the high and low pass filter parameters are systematically varied in real time to minimize a cost function. As the motion base moves closer to its physical limits, the filter parameters are adjusted to reduce the amount of additional motion commanded. As the motion base returns to its center, the digital filter parameters are adjusted to allow more motion [10, 11].

The last algorithm to be used extensively in flight simulation is the optimal algorithm [5, 12]. In the optimal algorithm a linear model of the vestibular system is used. A cost function is defined that includes terms that attempt to create the same motion sensation in the simulator as in the simulated aircraft, based on the linear model of the vestibular system. The cost function also includes terms that penalize motion of the simulator. The cost function is minimized by assuming random inputs for the specific forces and angular velocities coming from the simulated aircraft and solving the algebraic Riccati equation for the optimal linear acceleration and angular velocity of the motion base.

Typically, tilt coordination is used in the washout algorithms to represent steady state specific forces by rotating the motion base to align gravity with the total specific force vector of the simulated vehicle. A new tilt coordination control method was developed by Romano [13] for use with motion washout algorithms. Starting with the classical washout algorithm, the typical linear high-pass filters were removed from the algorithm and a linear model of the tilt coordination circuit was developed. A linear quadratic Gaussian regulator (LQGR) was developed that controls the tilt channel to minimize both commanded tilt rate and total motion base position.

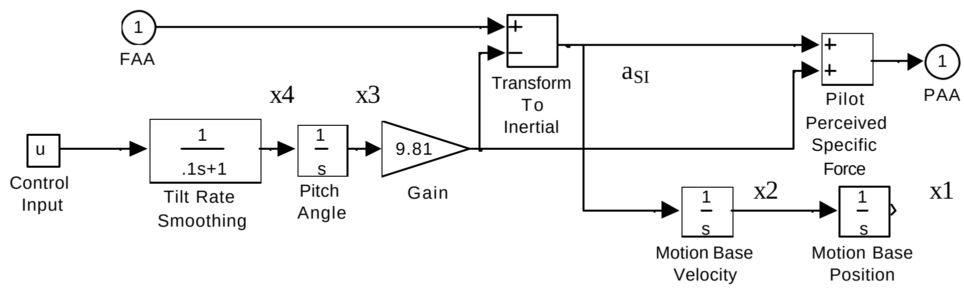

FIGURE 5 Linearized Algorithm

The new algorithm is shown in Figure 5. The control input u is tilt rate. The control input u is first smoothed using a first order lag and then integrated to yield a pitch angle. Tilt rate was selected as the control input u so that the maximum tilt rate can be controlled. If the output from the tilt rate smoothing is defined as the state x4, the integration of the pitch angle defined as x3, the velocity of the platform defined as x2, and the position is defined as x1, the algorithm can be represented using its equivalent state space representation.

$$\frac{d}{dt}\begin{bmatrix} x1 \\ x2 \\ x3 \\ x4 \end{bmatrix} = \begin{bmatrix} 0 & 1 & 0 & 0 \\ 0 & 0 & -9.81 & 0 \\ 0 & 0 & 0 & 1 \\ 0 & 0 & 0 & -1/c \end{bmatrix}\begin{bmatrix} x1 \\ x2 \\ x3 \\ x4 \end{bmatrix} + \begin{bmatrix} 0 \\ 0 \\ 0 \\ 1/c \end{bmatrix} u \tag{1}$$

A linear quadratic Gaussian regulator (LQGR) was selected [13] to calculate the control input u. To find an optimal solution the specific force input f_{AA} was treated as a white noise system disturbance filtered through a first order lag with a time constant of 0.05 seconds. While modeling the specific force as white noise is not exact, it makes the problem tractable. The state equation of the external input becomes:

$$\frac{d}{dt}[f_{AA}] = [-1/0.05][f_{AA}] + [0]u + w \tag{2}$$

where w is white noise. Kwakernaak [14] presented an approach to solve this type of problem. The original state equations in Equation 1 and the state equation in Equation 2 are combined to yield the augmented system given in Equation 3.

$$\frac{d}{dt}\begin{bmatrix} x1 \\ x2 \\ x3 \\ x4 \\ x5 \end{bmatrix} = \begin{bmatrix} 0 & 1 & 0 & 0 & 0 \\ 0 & 0 & -9.81 & 0 & 1 \\ 0 & 0 & 0 & 1 & 0 \\ 0 & 0 & 0 & -1/c & 0 \\ 0 & 0 & 0 & 0 & -20 \end{bmatrix}\begin{bmatrix} x1 \\ x2 \\ x3 \\ x4 \\ x5 \end{bmatrix} + \begin{bmatrix} 0 \\ 0 \\ 0 \\ 1/c \\ 0 \end{bmatrix} u + w \tag{3}$$

It is desirable to configure the linear quadratic regulator developed by Romano to control a tracking problem where the position state x1 is kept as close to zero as possible, the specific force state x5 is kept as close to the predefined specific force time history as possible and the control input u is minimized. In this case rather than assuming a white noise for the specific force input f_{AA}, a deterministic signal can be assumed. Therefore the white noise can be replaced with a second control input to allow control of the specific force input f_{AA}.

$$\frac{d}{dt}\begin{bmatrix} x1 \\ x2 \\ x3 \\ x4 \\ x5 \end{bmatrix} = \begin{bmatrix} 0 & 1 & 0 & 0 & 0 \\ 0 & 0 & -9.81 & 0 & 1 \\ 0 & 0 & 0 & 1 & 0 \\ 0 & 0 & 0 & -1/c & 0 \\ 0 & 0 & 0 & 0 & -20 \end{bmatrix}\begin{bmatrix} x1 \\ x2 \\ x3 \\ x4 \\ x5 \end{bmatrix} + \begin{bmatrix} 0 & 0 \\ 0 & 0 \\ 0 & 0 \\ 1/c & 0 \\ 0 & 20 \end{bmatrix} u \tag{4}$$

The desired tracking behavior is accomplished with the following cost function:

$$J = \int \left[[z-r]^T Q [z-r] + u^T R u \right] dt \tag{5}$$

where Q, R are weighting matrices, r is the desired command to track and:

$$\begin{bmatrix} z1 \\ z2 \end{bmatrix} = \begin{bmatrix} 1 & 0 & 0 & 0 & 0 \\ 0 & 0 & 0 & 0 & 1 \end{bmatrix}\begin{bmatrix} x1 \\ x2 \\ x3 \\ x4 \\ x5 \end{bmatrix} \tag{6}$$

The optimal solution to the linear tracking problem is [14]:

$$u^* = -R^{-1}B^T U x - R^{-1}B^T s \tag{7}$$

where U is the positive, semi-definite, symmetric solution to the Riccati equation:

$$\dot{U} = -UA - A^T U - D^T Q D + U B R^{-1} B^T U \tag{8}$$

and s is the solution of the co-state equations:

$$\dot{s} = -[A^T - UBR^{-1}B^T]s + D^T Q r \tag{9}$$

Finally:

$$A = \begin{bmatrix} 0 & 1 & 0 & 0 & 0 \\ 0 & 0 & -9.81 & 0 & 1 \\ 0 & 0 & 0 & 1 & 0 \\ 0 & 0 & 0 & -1/c & 0 \\ 0 & 0 & 0 & 0 & -20 \end{bmatrix} \tag{10}$$

$$B = \begin{bmatrix} 0 & 0 \\ 0 & 0 \\ 0 & 0 \\ 1/c & 0 \\ 0 & 20 \end{bmatrix} \tag{11}$$

$$D = \begin{bmatrix} 1 & 0 & 0 & 0 & 0 \\ 0 & 0 & 0 & 0 & 1 \end{bmatrix} \tag{12}$$

After some tuning Q and R were selected as:

$$Q = \begin{bmatrix} 0.005 & 0 \\ 0 & 1 \end{bmatrix} \tag{13}$$

$$R = \begin{bmatrix} 1 & 0 \\ 0 & 4 \end{bmatrix} \tag{14}$$

To solve the optimal control U and s were integrated from the end time back to the start time using Equations 8 and 9 and initial conditions:

$$U(t_f) = H \tag{15}$$

$$s(t_f) = -D^T H r \tag{16}$$

where:

$$H = \begin{bmatrix} 0.01 & 0 & 0 & 0 & 0 \\ 0 & 0 & 0 & 0 & 0 \\ 0 & 0 & 0 & 0 & 0 \\ 0 & 0 & 0 & 0 & 0 \\ 0 & 0 & 0 & 0 & 2 \end{bmatrix} \tag{17}$$

With U and s known, Equation 4 can be integrated forward to solve for the motion base position, acceleration and pitch angle.

The algorithm was first tested with a 2 m/s/s stopping maneuver. This test was performed to confirm the proper performance of the algorithm and to compare the new algorithm with the classical algorithm. The parameters in the classical algorithm were chosen such that similar tilt rates and motion base positions were achieved.

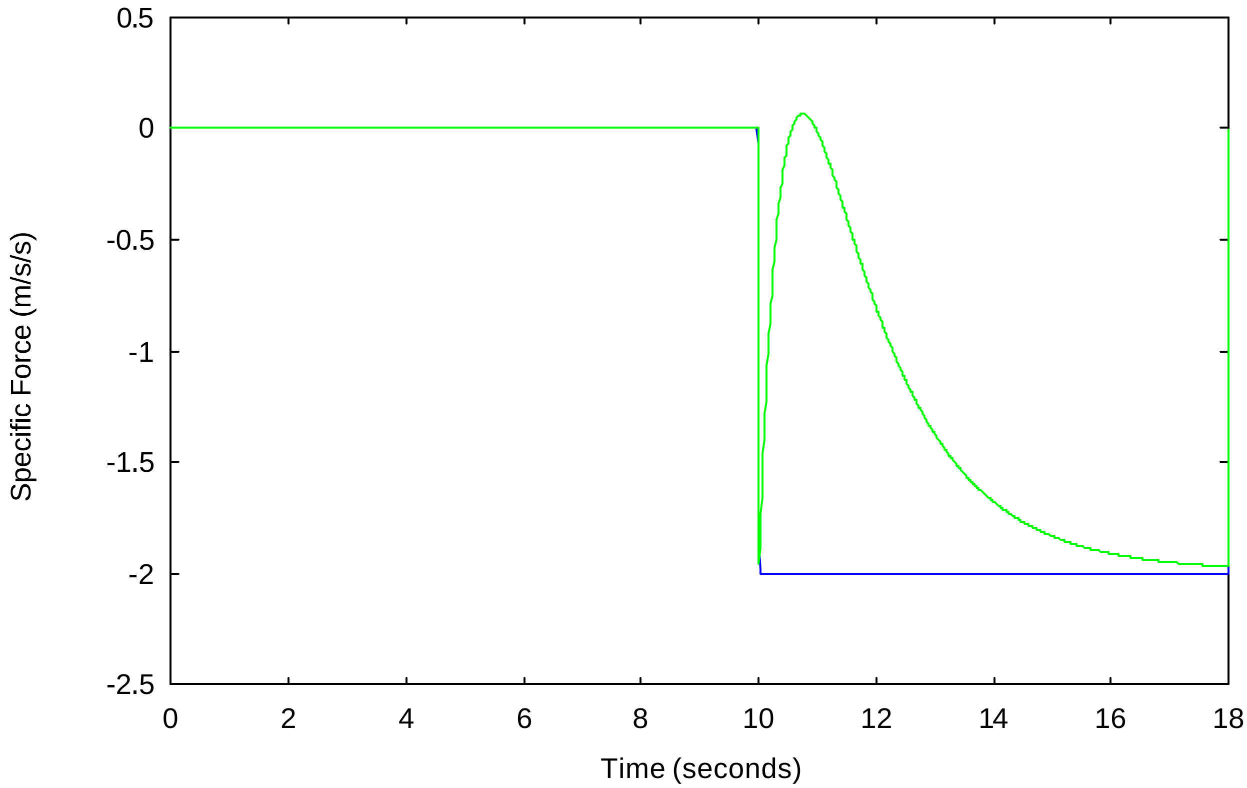

FIGURE 6 Specific Force Comparison

Figure 6 shows the response generated by the new algorithm in blue and the response of the classical algorithm in green. As can be seen in the figure the new algorithm produces very close to the true 2 m/s/s deceleration command. The classical algorithm shows a significant sagging cue. This is because for the classical algorithm the high pass filter generates the initial onset cue and the tilt coordination channel takes some time to ramp in the steady state specific force cue.

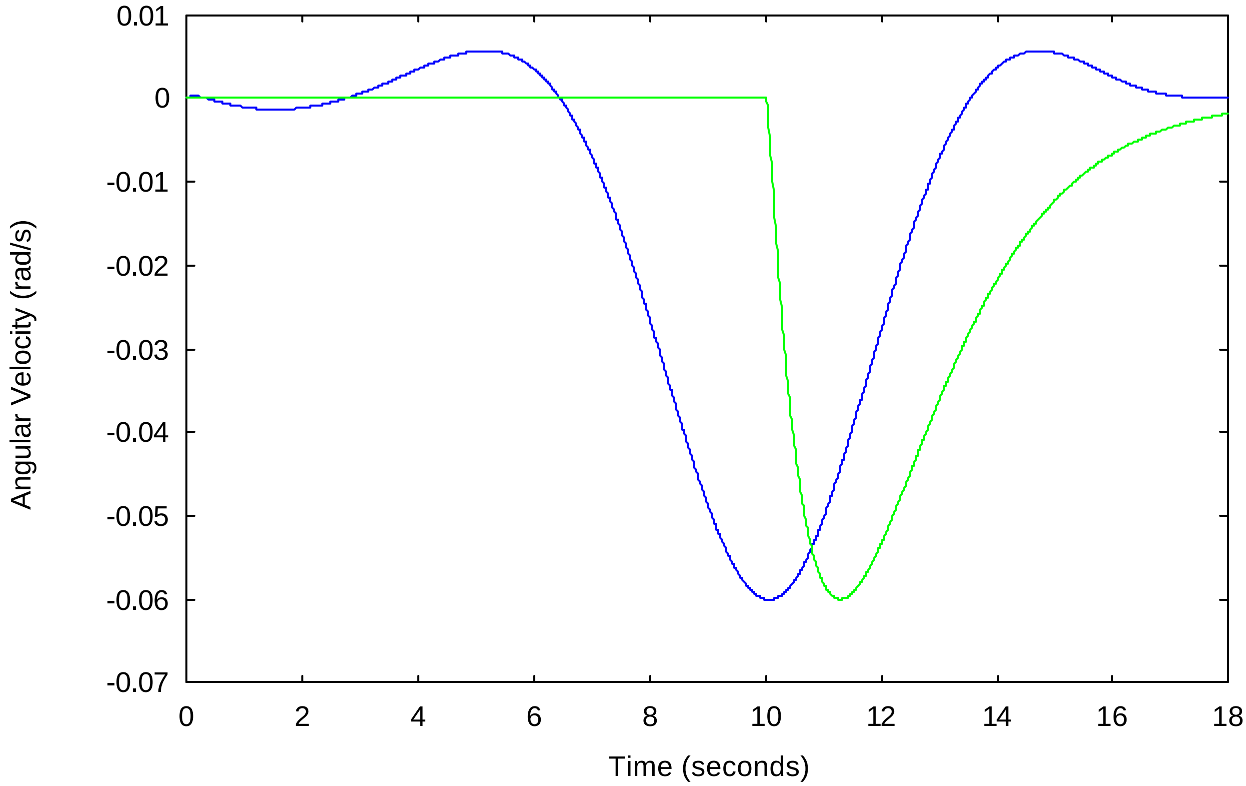

FIGURE 7 Tilt Rate Comparison

Figure 7 shows the tilt rates of the new algorithm and the classical algorithm. Again the new algorithm is in blue and the classical algorithm is in green. In this case one can see that the magnitudes of the tilt rates are very similar, however, the new algorithm ramps in the tilt rate far earlier. This is because the new algorithm can see ahead and knows when the braking maneuver will start.

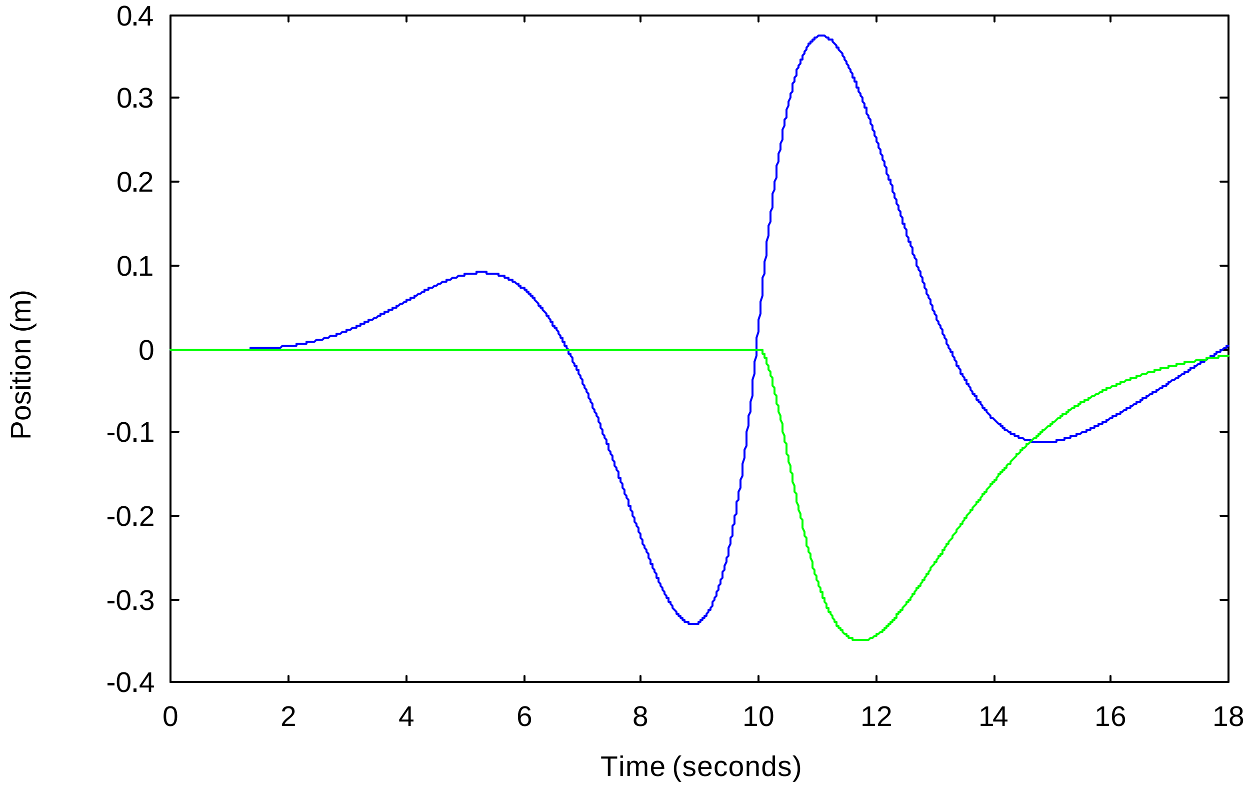

FIGURE 8 Position Comparison

Finally, Figure 8 shows the position comparison. Again the new algorithm is in blue and the classical algorithm is in green. Since the new algorithm can see when the braking maneuver will start, it ensures that the motion base will have a maximum positive velocity at the maneuver start point. In this way when the braking maneuver starts, the algorithm can generate a maximum negative acceleration of the motion base.

Based on this analysis it is clear that the algorithm is functioning well and outperforms the classical algorithm.

The algorithm was tested with a data set collected on the Aberdeen proving grounds. Figure 9 shows the results of the new washout algorithm compared with the real data. The blue graph is the response and the green graph is the original signal. From Figure 9, only the green signal is visible because the two signals overlay each other very closely.

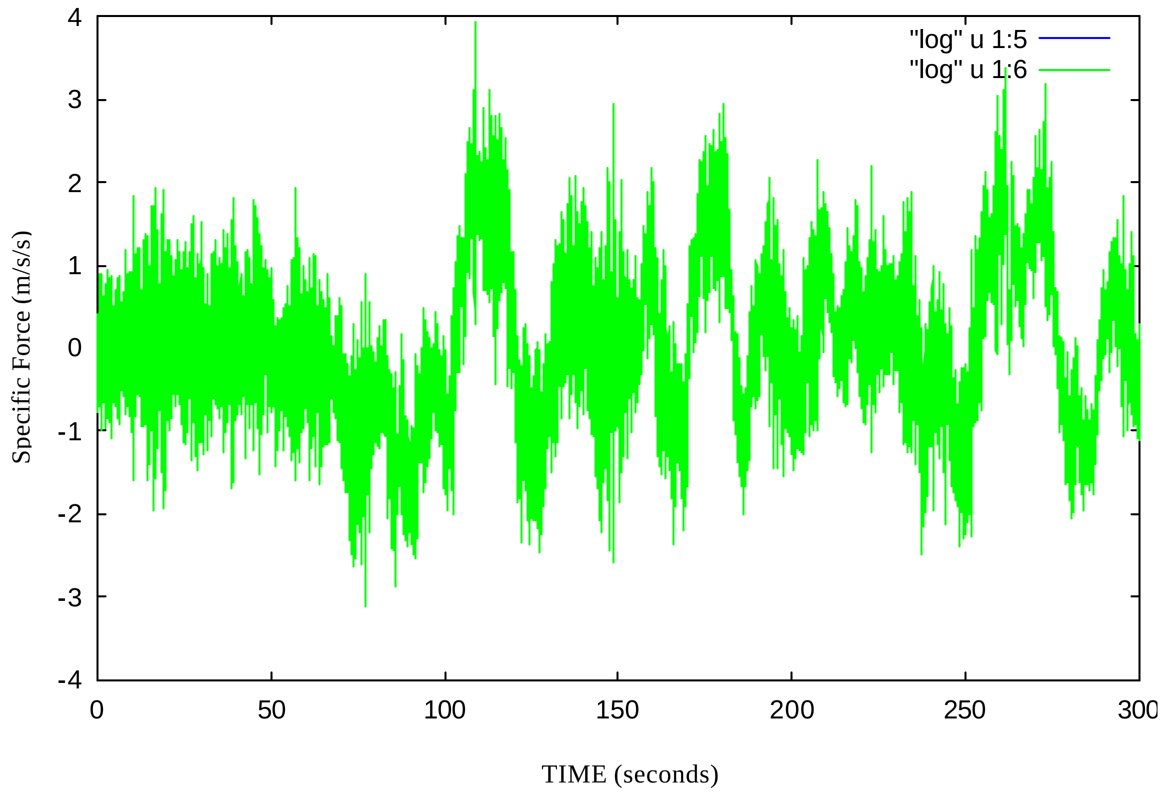

FIGURE 9 Specific Force Response of Algorithm

Figure 10 shows the same response zoomed in for the time from 25 to 26 seconds. Looking at the zoomed response there is a slight reduction in the total cue provided by the algorithm. This is because the cost function in Equation 5 will allow some reduction in the response as part of its total error calculation. Figure 11 shows the total tilt rate used by the algorithm. It can be seen that the tilt rate is maintained at less than 4 degrees/second (0.07 radians/second) for almost all the run and the tilt rate is typically well below 3 degrees/second. Finally Figure 12 shows the motion base position used by the algorithm. For most of the time the total motion base is kept below 0.3 meters which is well within the available limits of TACOM's RMS simulator.

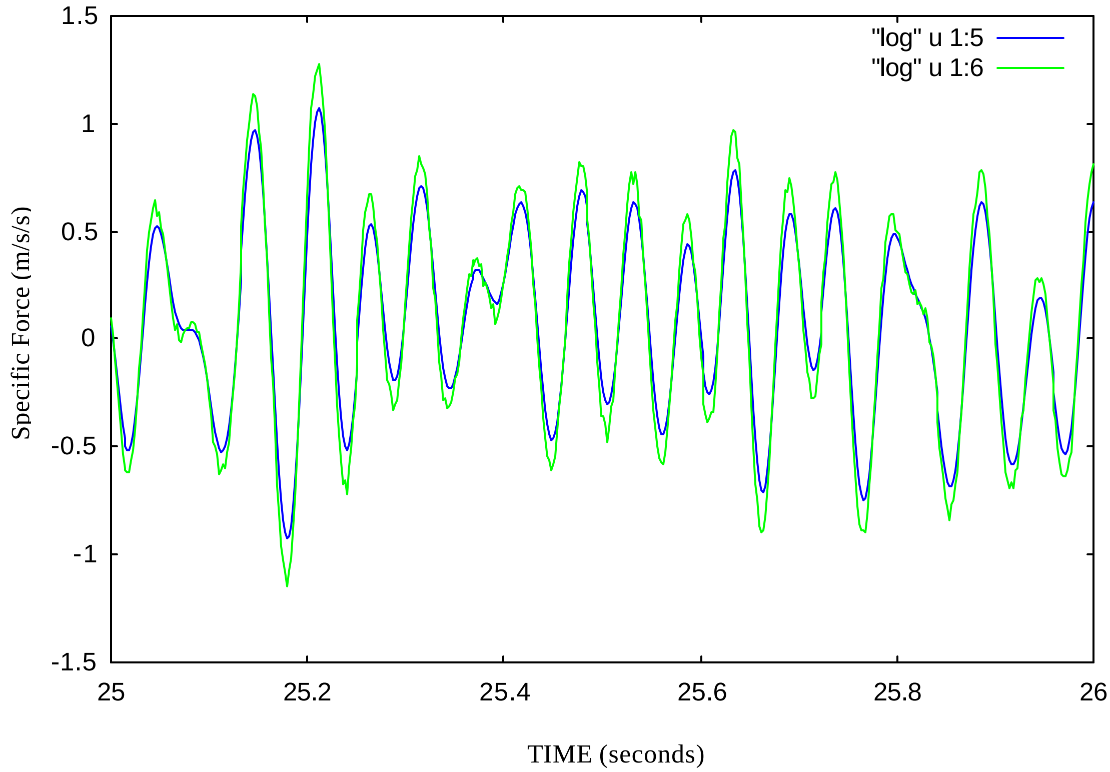

FIGURE 10 Zoom In of Specific Force Response of the Algorithm

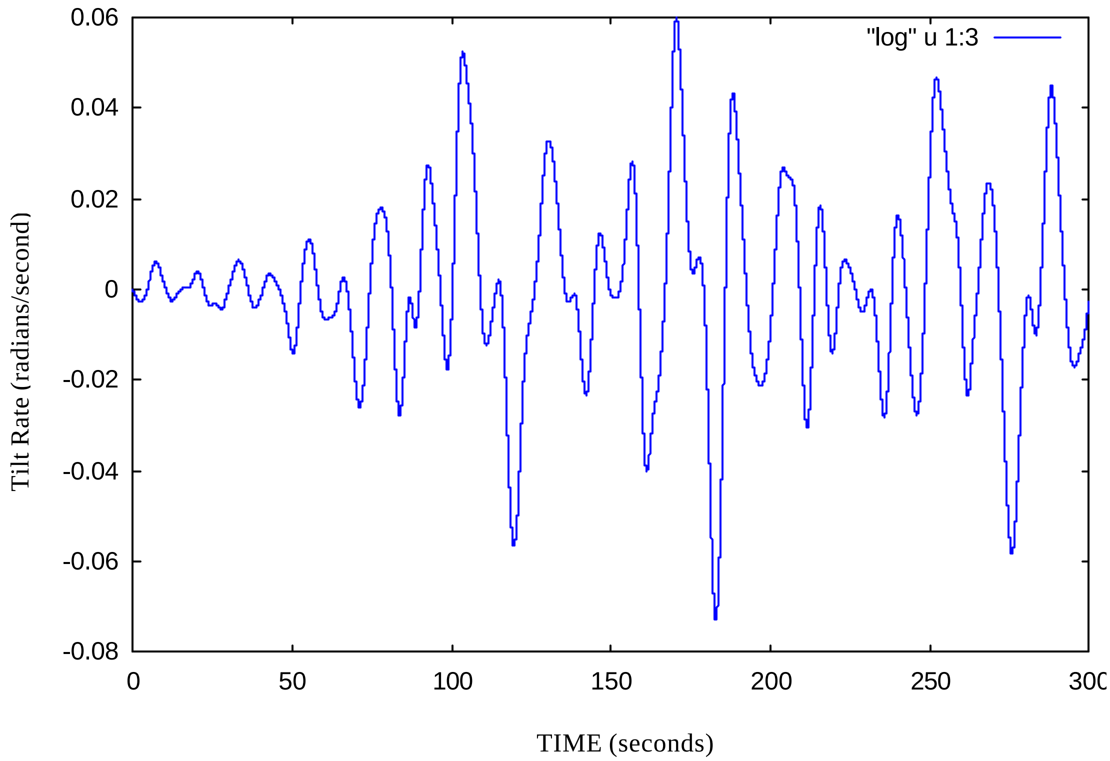

FIGURE 11 Tilt Rate Response of the New Algorithm

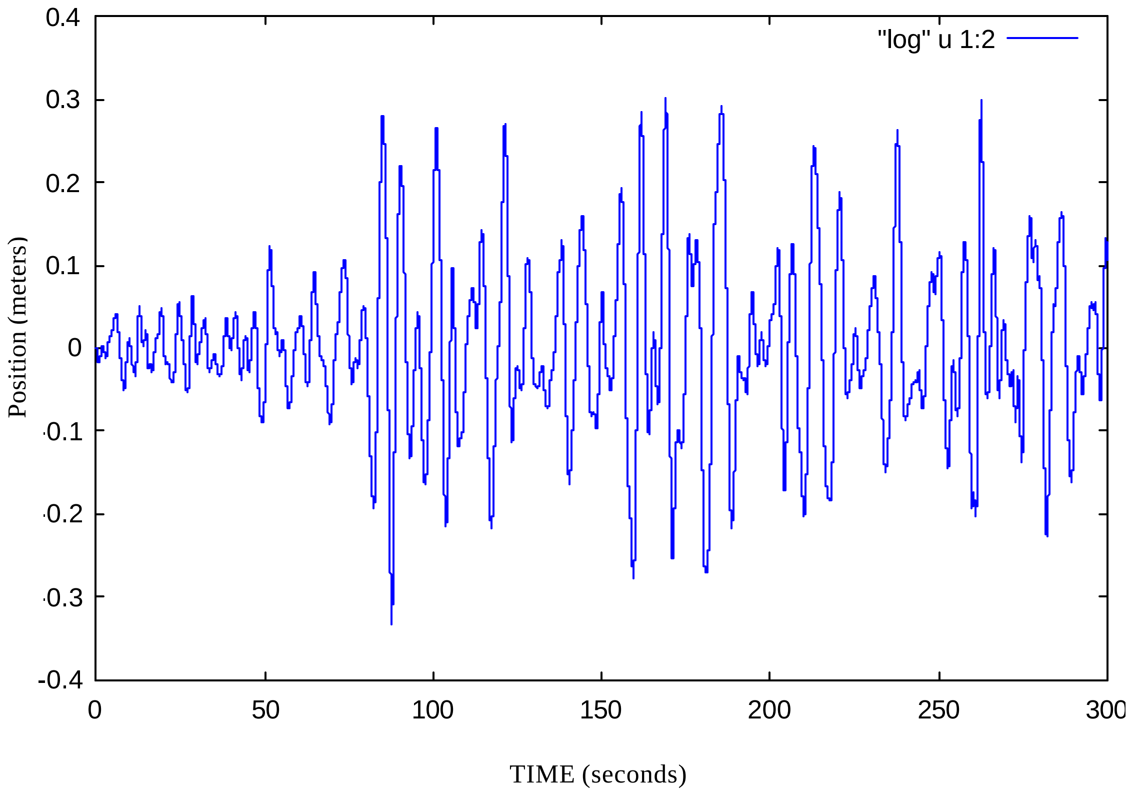

FIGURE 12 Position Response of the New Algorithm

CONCLUSION

Several experiment designs and ride simulator configurations are being considered for the study and investigation of moving vehicle operations and soldier performance. These designs will augment vehicle technology demonstrators and crewstation prototypes as these mature into production vehicles. In the future, motion sickness mitigation techniques can be tried in the simulator before more costly attempts are investigated. Caution must be exerted to decipher and determine the differences between simulator-caused sickness and motion sickness caused by poor vehicle designs.

A new motion washout algorithm was developed that converts prerecorded data into motion base position commands. Using prerecorded data an optimal set of tilt rate and acceleration commands can be developed that provides accurate specific force recovery while minimizing the total motion base envelope required.

Because the new motion washout algorithm has access to prerecorded data, the new algorithm outperforms a typical classical washout algorithm.

REFERENCES

1. Cowings P. S, Toscano, W. B., DeRoshia, C., & Tauson, R. A., "The Effects of the Command and Control Vehicle (C2V) on Soldier Health and Performance." Army Research Laboratory, 1999

2. Web site on the Future Combat System, http://www.darpa.mil/fcs/index.html

3. Nunez, P., Brudnak, M.J., Paul, V., "Warfighter/hardware in the Loop Simulation at TACOM-TARDEC's Ground Vehicle Simulation Laboratory (GVSL). In 1st Human Centered Transportation Simulation Conference, Iowa City, Iowa, 2001.

4. Tauson, R. A., "An Evaluation of the Effect of Ride Quality on Squad Performance.", Army Research Laboratory, 2002

5. Reid, L.D. and Nahon, M.A., "Flight Simulator Motion-Base Drive Algorithms: Part 1 – Development and Testing the Equations", UTIAS Report No. 296, University of Toronto, Ontario, Canada, 1985.

6. Schmidt, S.F., and Conrad, B., "A Study of Techniques for Calculating Motion Drive Signals for Flight Simulators," CR-114345, NASA, Mountain View, CA, July 1971.

7. Sinacori, J.B., "A Practical Approach to Motion Simulation," Paper No. 73-931, *Proceedings of the AIAA Visual and Motion Simulation Conference,* AIAA, New York, NY, September 1973.

8. Parrish, R.V., Dieudonne, J.E., and Martin, D.J. Jr., "Motion Software for a Synergistic Six-Degree-of-Freeedom Motion Base," TN D-7350, NASA, December 1973.

9. Baarspul, M., "The Generation of Motion Cues on a Six-Degrees-of-Freedom Motion System," Rept. LR-248, Dept. of Aerospace Engineering, Delft Univ. of Technology, Delft, The Netherlands, June 1977.

10. Parrish, R.V., Dieudonne, J.E., Bowles, R.L., and Martin, D.J., "Coordinated Adaptive Washout for Motion Simulators," *Journal of Aircraft*, Vol. 12, No. 1, January 1975, pp 44-50.

11. Kirdeikis, J., "Evaluation of Nonlinear Motion-Drive Algorithms For Flight Simulators," Technical Note No. 272 CN ISSN 0082-5263, University of Toronto Institute for Aerospace, June 1989.

12. Ish-Shalom, J., "The Design of Optimal Control Motion for Flight Simulators", Ph.D. Dissertation, M.I.T., Center for Space Research, Cambridge, MA, 1982.

13. Romano, R. A., "Non-Linear Optimal Tilt Coordination for Washout Algorithms", American Institute of Aeronautics and Astronautics, Modeling and Simulation Conference, Austin, Texas, 2003.

14. Kwakernaak, H., and Sivan, R., *Linear Optimal Control Systems*, Wiley-Interscience, New York, NY, 1972.